Dexmedetomidine — commonly used in resting-state and neurovascular coupling studies — is prone to inducing seizures in rats but not in wild type mice

Abbreviated title:
Dexmedetomidine is prone to inducing seizures in rats but not in wild type mice

Aleksandra Bortel, Ze Shan Yao, Amir Shmuel

Montreal Neurological Institute, McConnel Brain Imaging Centre
Departments of Neurology and Neurosurgery and Biomedical Engineering
McGill University, Montreal, QC, H3A 2B4, Canada

Correspondence to:
Aleksandra Bortel or Amir Shmuel
3801 University, room NW255
Montreal, QC, Canada H3A 2B4
Tel: +1-514-398-5943
Fax: +1-514-398-8106
E-mail: aleksandra.bortel@mcgill.ca, amir.shmuel@mcgill.ca

Keywords: dexmedetomidine, seizures, hemodynamic changes, CBF, primary somatosensory cortex, S1FL, peripheral somatosensory stimulation

Acknowledgements:
This study was supported by the Canadian Institute of Health Research (Grant MOP-102599) and the Natural Sciences and Engineering Research Council of Canada (RGPIN 375457-09 and RGPIN 2015-05103) awarded to A.S. We thank Roland Pilgram for the pipeline for analyzing electrophysiological data, and Jean Gotman, Massimo Avoli, Victor Mocanu and Pascal Kropf for their helpful technical advice and discussions.

ABSTRACT

Functional MRI (fMRI) of the resting-state utilizes spontaneous fluctuations in metabolic and hemodynamic signals to indirectly infer the underlying local changes in neuronal activity. For correct interpretation of spontaneous fluctuations and functional connectivity in the resting-state, it is important to characterize the neuronal mechanisms of fMRI in animal models. Animal studies of the evoked response and resting-state commonly use dexmedetomidine sedation. It has been demonstrated that dexmedetomidine combined with potent sensory stimuli is prone to inducing seizures in Sprague-Dawley (SD) rats.

To characterize these seizures, here we combined optical imaging of intrinsic signals and cerebral blood flow with neurophysiological recordings. We characterize the susceptibility to seizures as a function of time from the beginning of dexmedetomidine administration. We show that these seizures are associated with spatially extensive high-amplitude cerebral blood flow and blood oxygenation responses, prone to be misinterpreted as normal responses in functional imaging studies that do not use neurophysiological recordings. We demonstrate that such seizures are generated not only in SD rats but also in Long-Evans rats. In contrast, we did not observe any seizures in C57BL6 mice that were similarly sedated with dexmedetomidine and stimulated with similar potent stimuli.

We conclude that caution should be practiced in experiments that combine the administration of potent stimuli with dexmedetomidine sedation because high-amplitude hemodynamic responses evoked by peripheral stimulations are possibly due to the induction of epileptic activity in the cortical brain area. We further conclude that the susceptibility to dexmedetomidine-induced seizures is species dependent.

INTRODUCTION

Functional connectivity (FC) refers to the temporal correlation between spatially remote neurophysiological events (Friston et al., 1993). FC analysis based on functional magnetic resonance imaging (fMRI) makes it possible to obtain an approximation of the pattern of thalamocortical and cortico-cortical connections noninvasively, thus it is readily usable on human subjects. FC analysis can be pursued using data obtained during subject stimulation, task performance, or in the resting-state. In addition to shedding light on the pattern of connections, FC carries information that can be used to detecting malfunction of the brain in disease (Fox and Greicius, 2010).

fMRI of the resting-state utilizes spontaneous fluctuations in metabolic and hemodynamic signals to infer the underlying local changes in neuronal activity (Shmuel and Leopold, 2008). Thus, the fMRI signal is an indirect measure of changes in neuronal activity. Therefore, for correct interpretation of spontaneous fluctuations and FC in the resting-state, it is important to characterize the neuronal mechanisms of these phenomena by combining fMRI and neurophysiology in animal models.

Animal studies of the resting-state commonly use dexmedetomidine, which results in sedation rather than deep anesthesia. Dexmedetomidine has been the anesthetic of choice for long functional imaging studies in rats (Fukuda et al., 2013; Nasrallah et al., 2012; Pawela et al., 2008; Sotero et al., 2010; Zhao et al., 2008) and mice (Adamczak et al., 2010; Bukhari et al., 2017).

It has been reported that medetomidine sedation does not affect seizure vulnerability, nor does it affect LFP and BOLD responses during seizures evoked by systemic administration of kainic acid in rats (Airaksinen et al., 2012; Airaksinen et al., 2010). In contrast, Fukuda et al. (2013) demonstrated that sedation induced by intravenous perfusion of dexmedetomidine for more than two hours changes seizure susceptibility in rats. Accordingly, forelimb stimulation elicited seizure-like responses accompanied by changes in cerebral blood flow (CBF) in Sprague-Dawley (SD) rats (Fukuda et al., 2013). These results have been corroborated by Bortel et al. (2019), who characterized the pattern of seizures and demonstrated that the determining factors for inducing the seizures are the administration of dexmedetomidine combined with potent sensory electrical stimulation. Indeed, dexmedetomidine sedation alone, even if combined with short and weak peripheral stimulation is not sufficient for inducing epileptiform activity (Sotero et al., 2015). However, potent stimulations in the range of 9-12 Hz are commonly used for imaging under medetomidine, isoflurane, or urethane anesthesia as these frequencies elicit the strongest BOLD response (Huttunen et al., 2008; Kim et al., 2010; Krautwald and Angenstein, 2012; Masamoto et al., 2007; Zhao et al., 2008). Therefore, it is important to test whether these stimuli influence the hemodynamic responses that are the basis for fMRI. Moreover, mice sedated with dexmedetomidine are commonly used for studying the mechanisms underlying neurovascular coupling and resting-state fMRI. However, whether dexmedetomidine induces seizures in mice remains unknown.

Here we report on the dependence of dexmedetomidine-induced seizures in SD rats on time of dexmedetomidine administration. We demonstrate that the seizures are accompanied by spatially extended cerebral blood flow and blood oxygenation responses. We further show that under dexmedetomidine sedation, forepaw stimulation induces seizures not only in SD rats but also in Long-Evans (LE) rats. In contrast, C57BL6 (C57) wild type mice do not show susceptibility to seizures under the same sedation regime and stimulation protocol. We conclude that experiments using potent sensory stimuli and dexmedetomidine sedation in SD and LE rats are prone to generating seizures accompanied by extended hemodynamic responses.

MATERIALS AND METHODS

Animals and surgical procedures

All procedures were approved by the animal care committees of the Montreal Neurological Institute and McGill University and were carried out in accordance with the guidelines of the Canadian Council on Animal Care. Here we report on experiments performed on 6 adult (100–107 days old) male SD rats weighing 440–560 g, 5 adult (100–109 days old) male LE rats weighing 475–495 g, and 5 adult age-matched C57 mice weighing 30-37g. The rats and mice were housed

under the same controlled environmental conditions at 22±2º C with a 12h light/12h dark cycle (lights on from 7:00 a.m. to 7:00 p.m.) and received food and water ad libitum. A brief description of the surgical procedures is included below. All procedures carried out for experiments in SD rats are described in detail in Bortel et al. (2019). The procedures applied for experiments in LE rats were identical to those used for experiments in SD rats.

The rats were initially anesthetized with a solution of xylazine (10 mg/kg IP; Bayer Inc., Canada) and ketamine (50 mg/kg IP; Wyeth, Canada). They were then intubated and placed in a stereotaxic frame. The surgical procedure was performed under ventilation with 100% oxygen and anesthesia with isoflurane (0.6-2%; Benson Medical Industries Inc., Canada). The scalp was incised to expose the skull covering the primary somatosensory cortex (S1) of the left hemisphere. One stainless steel screw (2.4 mm in length) used as a ground and reference, was fixed to the skull above the visual cortex of the right hemisphere. The part of the skull overlying S1 was thinned until soft and transparent. We then performed an approximate 4 mm wide square-shaped craniotomy, centered on the forelimb representation in area S1FL based on a stereotaxic atlas (AP 0.00 mm, ML ±4.50 mm, DV –2.5 mm; Paxinos and Watson, 2005). The dura mater within the craniotomy was resected. At the end of the surgical procedure, a silicon chamber was created around the craniotomy and filled with Hank's Balanced Salt Solution (Invitrogen, Canada).

Following the surgery, prior to starting the recordings, we changed the ventilation of the animal to a mixture of 20% oxygen and 80% medical air. At the same time, we injected a single dose of buprenorphine (0.04 mg/kg, SC; Schering-Plough, UK) and started perfusion of dexmedetomidine (0.075 mg/kg/h, SC; Pfizer Inc., Canada) that remained continuous throughout the recordings. The isoflurane administration was stopped following the administration of dexmedetomidine and buprenorphine.

The forepaw representation of area S1FL was delineated by optical imaging of the cerebral blood volume (CBV) response to forepaw stimulation. Then a linear multi-contact probe was inserted into the forepaw representation of area S1FL.

To determine the effect of dexmedetomidine on seizure susceptibility in a different animal species, we performed similar procedures and the same type of forepaw stimulation in five age-matched mice. The surgical procedure was performed under anesthesia with a solution of ketamine (100 mg/kg IP; Wyeth, Canada) and xylazine (10 mg/kg IP; Bayer Inc., Canada). The core temperature and heart rate were monitored. The primary somatosensory cortex (S1) of the left hemisphere was exposed, by performing a craniotomy, centered on the forelimb representation in area S1 (S1FL) based on a mouse stereotaxic atlas (AP -0.30 mm, ML ±2.20 mm, DV –1.3 mm; Franklin and Paxinos (2007). Following the surgery, prior to starting the recordings, the mice were injected with a single dose of buprenorphine (0.1 mg/kg, SC; Schering-Plough, UK) and continuously perfused with dexmedetomidine (0.05 mg/kg/h, SC; Pfizer Inc., Canada). Then, a linear multi-contact probe was inserted into area S1FL. To maintain the sedation throughout the experiment, we infused dexmedetomidine continuously at a rate of 0.05 mg/kg/h SC. We assessed the depth of sedation by continuously monitoring the vital signs of the animal and by monitoring whether the animal stayed still or performed any movement. In case this monitoring showed that

additional sedation was required, we increased the rate of the dexmedetomidine infusion to 0.1 mg/kg/h SC.

Electrical stimulation of the forepaw

Electrical stimuli were generated using a stimulator/isolator (A365, WPI, Sarasota, FL) and delivered through two needle electrodes inserted into the web spaces of digits 2/3 and 4/5 of the rat or mouse forepaw. With rats and mice, we began our experiments with optical imaging of area S1FL, in order to guide the insertion of the neurophysiology probe to the forepaw representation. Runs for eliciting CBV-based optical imaging responses consisted of ten 4s stimulation blocks of 1 ms long, 1 mA electrical current pulses delivered at a frequency of 8 Hz. Following the insertion of the probe, we obtained data for the main experiment, including LFP, and HbO and CBF responses to electrical stimuli delivered to the forepaw. In rats, 8 runs were performed, each consisting of ten 35s-long stimulation trials, separated by ten 35s-long trials in which no stimulus was delivered (see time course in Figure 1A). Each stimulation trial started with 5s recordings of baseline activity, followed by 10s of stimulation and 20s of baseline activity. Each 10s stimulation block consisted of a train of 1 ms long, 2 mA electrical pulses delivered at a frequency of 8 Hz. In mice, 9 similar runs were performed, except that three different stimulus frequencies (4Hz, 6Hz, and 8Hz) were applied. The recordings were performed in runs with increasing (3 mice) or decreasing (2 mice) stimulation frequency. The duration and intensity of all electrical pulses delivered to mice were identical to those delivered in rats. In all experiments in rats and mice, the polarity of stimulation was switched in each pulse relative to the polarity of the preceding pulse.

Optical imaging of intrinsic signals

All procedures applied for optical imaging of intrinsic signals (OIS) are described in detail by Bortel et al. (2019). The ROI we imaged was centered on the atlas coordinates of area S1FL in the left hemisphere in rats (AP 0.00 mm, ML ±4.50 mm, DV –2.5 mm; Paxinos and Watson (2005)) and mice (AP -0.30 mm, ML ±2.20 mm, DV –1.3 mm; Franklin and Paxinos (2007)). We imaged the hemodynamic responses to forepaw stimulation at a frame rate of 30 Hz. under the illumination of a green and orange LED light with a center wavelength of 530 nm (isosbestic point) and 617 nm, respectively.

Laser Speckle flowmetry

One laser Speckle (Sharp LTO25MD; λ = 798 nm, 30 mW; Thorlabs, Newton, NJ, U.S.A.) diode was coupled into a 600-µm diameter silica optical fiber (Thorlabs FT600-EMT) and a collimating lens (f = 8 mm, C240-TM; Thorlabs) was connected to the distal end of the fiber. The lens was placed approximately 10 cm above the cortical ROI. It was adjusted to provide even illumination over an area with 8 mm diameter on the exposed cortical surface. The coherence length of the laser was approximately 1 cm. The speckle pattern was imaged using a CCD camera (Teledyne Dalsa, Waterloo, Ontario, Canada), which made it possible to obtain 2D maps of CBF at high spatial and temporal resolution. To this end, we quantifying the spatial blurring of the speckle pattern that

results from blood flow (Boas and Dunn, 2010). Conversion of the raw speckle images to blood flow maps was done using custom-written software that computed the speckle contrast and correlation time values at each pixel (Dunn et al., 2001).

Electrophysiological data preprocessing and seizure analysis

The methods used for the pre-processing of electrophysiological data and seizure analysis are specified in detail in Bortel et al. (2019).

Statistical evaluation

We used the Levene's test to examine whether the variances of two or more compared groups were equal. In the cases where equal variances were verified, a Student's t-test was performed to test differences in the means of two groups. If there was evidence to support non-equal variances, a one-way ANOVA post hoc Tamhane's test was applied to evaluate statistical differences between the groups. A nonparametric Wilcoxon test was applied to groups of paired data variables. Results are presented as a mean ± SEM. Differences with $p < 0.05$ were considered statistically significant (IBM SPSS Statistics, 2016).

RESULTS

Characterization of normal evoked and epileptic responses

Typical LFP patterns recorded during normal evoked responses in area S1FL of an SD rat are presented in Figures 1A (trials 2, 3, 5, 6, 8, 9, and 10) and 1B. The normal evoked responses were confined within the 10s period of stimulation. As illustrated in Figure 1B, the LFP amplitudes in response to electrical stimulation pulses were higher than the spontaneous LFP amplitudes. In four of six rats, we detected seizures induced by somatosensory stimulation of the forepaw. Figures 1A (trials 1, 4, and 7) and 1C present seizures induced by the forepaw stimulation. As can be observed in Figure 1C, the onset of the seizure (marked by a red arrow) consisted of high-frequency negative or positive-going deflections of the mean extracellular field potential.

The seizures typically extended for several seconds longer than the stimulation period. Before they terminated, the seizures consisted of low-frequency, high amplitude deflections of the field potential, extending above or below the baseline (Figure 1C; the seizure end is marked by a green arrow). The LFP and the corresponding spectrograms were used to estimate the seizure onset and termination times, relative to the first stimulation pulse. All seizures evoked in our rats were brief, lasting less than one minute. The average duration of seizures was 31.50 ± 1.83s. The seizures were followed by another seizure (55 cases out of 113 seizures), or a refractory period (40 refractory periods out of 113 seizures) or a normal response (14 normal responses out of 113 seizures).

The first recording run was performed 15 min after the isoflurane administration was stopped, thus 30 min following the administration of dexmedetomidine and buprenorphine. In the first 10-min run we stimulated the forepaw for eliciting CBV-based optical imaging responses (4s stimulation

blocks, administering 1 mA pulses at 8 Hz). We did not observe any epileptic activity during this first stimulation run. Approximately 40 min following the administration of dexmedetomidine and buprenorphine, prior to the stimulation runs, we acquired two 10 min long runs of spontaneous activity. We did not observe any epileptic activity during these runs. These findings indicate that dexmedetomidine alone does not induce seizures: potent stimuli are required too, for the seizure generation.

Seizures were observed already during the first or the second stimulation run in which we applied 10s stimulation of 2 mA pulses at 8 Hz (Figure 1D), after one hour of dexmedetomidine perfusion. In SD rats, the average number of observed seizures during the period of 60-120 min following the initiation of dexmedetomidine sedation (6.2±0.8, median equal 6) was larger than the corresponding number observed during the period of 120-180 min following this initiation (3.5±0.6, median equal 4; p=0.12, Wilcoxon test; non-significant trend).

The seizures induced in SD rats by electrical forepaw stimulation were exclusively electrographic seizures. We did not observe any physiological epileptic behavior in our sedated rats.

Seizures induced by dexmedetomidine are associated with extended cerebral blood oxygenation and flow

To test how the seizures induced by forepaw stimulation under dexmedetomidine sedation influence hemodynamic responses, we analyzed the spatial extent of the hemodynamic responses elicited during normal evoked responses and seizures. Figures 2A-B and 3A-B present the spatial HbO and CBF responses, respectively, 1s before the stimulus onset (1), 10s after the stimulus onset (2), and 20s after the stimulus onset (3), for normal evoked response and seizure recorded in a single trial in one animal.

The spatial extent of the cerebrovascular hemodynamic responses 10s following the onset of stimulation was slightly larger during a seizure (Figure 2B and 3B, panel 2) than during a normal response (Figure 2A and 3A, panel 2). The spatial extent of the responding region 10s following the cessation of the stimulus was substantially larger during a seizure (Figure 2B and 3B, panel 3) than during a normal response (Figure 2A and 3A, panel 3). The timecourses of the HbO and CBF changes during a normal evoked response and an induced seizure response are presented on the right panels of Figures 2A-B and 3A-B, respectively. Two different colored lines correspond to the two brain regions marked in Figures 2C. At any time-point following the onset of the stimulus, the HbO and CBF amplitudes during the seizure (Figure 2B and 3B) were higher than the corresponding amplitudes during the normal evoked response (Figure 2A and 3A). The bar plot in Figure 3C presents the spatial extent of the CBF responses averaged over six animals, during normal responses, seizures and refractory periods, respectively. For each of the stimulation periods of 5–10s, 10–15s, and 15–20s relative to the onset of the stimulus, the spatial extent of the cerebrovascular hemodynamic changes during seizures was larger than during normal evoked responses and refractory periods (Figure 3C; * $p < 0.05$, ** $p < 0.001$, Tamhane's test). Note that the two latter periods, namely 10–15s and 15–20s relative to the onset of the stimulus, are part of the post-stimulation period in which the seizures persist with no sensory stimulation. Interestingly,

not only the average spatial extent of the seizures was larger than that of normal responses obtained during the same period following the cessation of the stimulus, also the seizure's spatial extent *post-stimulation* was larger than that observed in normal responses *during stimulation* (Figures 3C; $p < 0.001$, Tamhane's test). Thus, the seizures we induced propagated beyond the spatial extent of the normal responses to forepaw stimulation.

The susceptibility to seizures depends on animal species

The susceptibility of the brain to seizure generation is known to depend on animal species (Schauwecker, 2002). Therefore, we pursued the same experiment using another rat strain, namely the Long-Evans rat, and another rodent species, the C57BL6 mouse. Just like SD rats, LE rats and C57BL6 mice are commonly used in studies of the resting state and neurovascular coupling.

The LFP characteristics of seizures evoked in LE rats by forepaw stimulation under dexmedetomidine and buprenorphine sedation were similar to those evoked in SD rats (Figure 4A-D). Seizures induced in LE rats were observed as soon as one hour of dexmedetomidine perfusion, during the first or third stimulation run in which we applied 10s stimulation of 2 mA pulses at 8 Hz (Figure 4D). The average number of seizures during the period of 60-120 min following the initiation of dexmedetomidine sedation (median equal 6) was not statistically different than the corresponding number observed during the period of 120-180 min following this initiation (median equal 5; $p=0.55$, Wilcoxon test). The seizures were followed by another seizure (72 cases out of 149 seizures), or a normal response (60 normal responses out of 149 seizures), or a refractory period (16 refractory periods out of 149 seizures; Figure 4A-C). Lastly, the percentage of LE rats that showed seizures during forepaw stimulation (100%) was higher than the corresponding percentage in SD rats (67%).

In pilot experiments in 2 mice, we did not observe seizures and not even high-amplitude field responses to electrical stimuli administered at 8 Hz with parameters identical to those that elicited high-amplitude responses in SD and LE rats. We hypothesized that the reason for the lack of high-amplitude responses was that the inhibition elicited by the response in mice remains effective for a longer duration than it does in rats. In addition, low frequency of 6 Hz, 3s corneal stimulation produces 'psychomotor' seizures in mice (Barton et al., 2001; Esneault et al., 2017). Based on these observations, we decided to administer forepaw stimuli to five age-matched mice using three different frequencies of stimulation: 4Hz, 6Hz, and 8Hz. Figure 5A and B present normal responses obtained with 4Hz and 6Hz stimulation, respectively. Note that the normal responses are noticeable with the lowest stimuli frequency and are substantially weaker with 6Hz stimulation. The LFP responses to the forepaw stimulation of 8 Hz were virtually undetectable (Figure 5C). As illustrated in Figure 5A-C, we did not evoke any seizures with forepaw stimulation with any of the stimulation frequencies we administered to any of the mice under dexmedetomidine and buprenorphine sedation. Seizures were observed in SD and LE rats, but not in C57 mice.

DISCUSSION

Dexmedetomidine induces seizures in response to potent stimuli

Dexmedetomidine is an α2-adrenergic agonist predominantly acting on presynaptic receptors in the locus coeruleus. It regulates central adrenergic function and in consequence induces cerebral vasoconstriction mediated by direct agonist binding to receptors on the cerebral vessels resulting in reduced baseline of CBF and CBV (Adamczak et al., 2010; Jonckers et al., 2015; Paasonen et al., 2018; Pawela et al., 2009; Weber et al., 2006). The degree of vasoconstriction depends on the dose and delivery method (topical vs. systemic) (Jonckers et al., 2015). Dexmedetomidine decreases noradrenaline release (Gertler et al., 2001), which in turn decreases seizure threshold (Oishi and Suenaga, 1982). There have been many conflicting reports showing the influence of dexmedetomidine on seizure generation. It was shown, that the seizure frequency and onset time evoked by kainic acid (Airaksinen et al., 2012; Airaksinen et al., 2010) or pilocarpine (Choy et al., 2010) are similar in the awake and medetomidine-sedated rats. Halonen et al. (1995) demonstrated that rat convulsions induced by kainic acid are prevented by the administration of dexmedetomidine. Similarly, it was shown that rat seizures induced by administration of cocaine were supressed by dexmedetomidine sedation (Whittington et al., 2002). Furthermore, dexmedetomidine effectively decreases the number and cumulative time of repeated seizures evoked by prolonged electrical stimulation of the amygdala in experimental models but only at high doses of 100 μg/kg or higher (Kan et al., 2013). In contrast, it was shown that dexmedetomidine increases the epileptiform activity in epileptic patients (Chaitanya et al., 2015). In addition, dexmedetomidine exerts a significant proconvulsant action in the pentylenetetrazol seizure animal model. The proconvulsant effect is dose-dependent and stereospecific and is blocked by the selective α2-adrenergic antagonist atipamezole (Mirski et al., 1994). Likewise, Fukuda et al. (2013) demonstrated that epileptic activity can be induced in rats by electrical stimulation of the forelimb under continuous IV infusion of dexmedetomidine lasting more than two hours (Fukuda et al., 2013). In line with the findings by Whittington et al. (2002) and Airaksinen et al. (2012), we did not observe any seizure-like responses to short and weak forelimb stimuli (1s-long, 0.6-0.8 mA current pulses delivered at 8 Hz) under dexmedetomidine sedation (Sotero et al., 2015). Nevertheless, under the same anesthesia regime, long (10 s), frequent (8Hz) and potent (2 mA) peripheral electrical stimuli evokes seizures (Bortel et al., 2019). Similar potent peripheral stimulation in the range of 8-12 Hz and 1.5-2 mA is commonly used to elicit BOLD signal in dexmedetomidine sedated rodents.

In patients affected by Touch Induced Seizures (TIS), the sensory stimulations that induce seizures are repetitive and last 5-20 seconds (Hsieh et al., 2011; Kanemoto et al., 2001; Sala-Padro et al., 2015; Wolf, 2015). To trigger the epileptic activity in our animals, we applied a similar somatosensory stimulation. The electrical stimuli we delivered to the forepaw were repetitive and lasted 10 seconds. Epileptic activity induced in our rats consisted of brief and focal electrographic seizures that were followed by a refractory period, normal response, or another seizure and the animals did not show any epileptic behavior. Similarly, TIS manifests as focal, brief seizures frequently followed by a refractory period with no impairment of consciousness (Deonna, 1998;

Hsieh et al., 2011; Sala-Padro et al., 2015; Striano et al., 2012) and may have only electrographic display without any overt clinical manifestations (Panayiotopoulos, 2005).

Mechanisms of dexmedetomidine-induced seizure generation

We acknowledge that we did not perform systematic experiments to test the effect of dexmedetomidine dose on the susceptibility to seizure. Therefore, we cannot rule out that the susceptibility to the generation of seizures depends on the dose of dexmedetomidine. However, we obtained data that indicate that the lack of seizures in C57 mice did not depend on the dose. To maintain proper sedation in three of the mouse experiments, we had to increase the rate of dexmedetomidine from 0.05 mg/kg/h to 0.1 mg/kg/h approximately 80 minutes after the infusion started. However, no seizures were observed in these mice or in the other mice. These results are consistent with Fukuda et al. (2013)'s findings that increasing the dexmedetomidine IV infusion rate from 0.05 mg/kg/h to 0.15 mg/kg/h in SD rats does not change the susceptibility to seizure generation.

It is widely accepted that anesthetics modify the balance between excitation and inhibition towards increased relative inhibition, and consequently, they modulate evoked neuronal responses (Franceschini et al., 2010). Isoflurane is a general anesthetic that affects many neurotransmitter systems; it acts on GABA, NMDA, and glycine receptors (Grasshoff et al., 2006). Although isoflurane reduces neuronal excitation and cerebral metabolism, it is commonly used in electrophysiology studies. However, at higher doses (≥1.6%) isoflurane increases the baseline cerebral blood flow (CBF) (Eger, 1984; Franceschini et al., 2010) and for this reason, it is no longer the anesthetics of choice for hemodynamics-based functional studies. Therefore, to evaluate the dependence of the seizure generation on the anesthesia regime other than dexmedetomidine sedation, we performed six experiments using urethane (Bortel et al., 2019). Urethane is an anesthetic that has modest effects on both the inhibitory and excitatory systems and does not affect the noradrenergic system (Hara and Harris, 2002). The changes it exerts on multiple neurotransmitter-gated ion channels are much smaller than those seen with anesthetics more selective for one neurotransmitter system, such as ketamine. Therefore, urethane is suitable for maintaining anesthesia during electrophysiological recording (Hara and Harris, 2002). We previously applied the exact same experimental and forepaw stimulation procedures under urethane anesthesia (Bortel et al., 2019). Under urethane anesthesia, we did not evoke any seizures. We refer the reader to the detailed results of these experiments in Bortel et al. (2019).

Dexmedetomidine induced seizures are species-dependent

Previous works have demonstrated that the rat and mouse strains show diverse susceptibility to seizure-induction following systemic convulsant injection (Ferraro et al., 1995; Golden et al., 1995; McKhann et al., 2003). It was shown that the C57BL6 mouse strain has low seizure sensitivity and the DBA/2J and FVB/N strains high seizure sensitivity (Ferraro et al., 2002; Frankel et al., 2001). Our results confirm that seizure susceptibility depends on the animal's species and that sedating C57 mice with dexmedetomidine does not induce seizures.

Our findings demonstrate the lack of significant sustained LFP responses to 8Hz — and only reduced LFP responses to 6HZ — relative to responses to 4Hz forepaw stimulation in mice (Fig. KL). The maintenance of the proper balance between excitation and inhibition is critical for the normal function of cortical circuits (Turrigiano, 2011). This continuum of changes in response amplitude suggests that changes in the balance between excitation and inhibition take place as a function of the stimulation frequency. We propose that the inhibitory tone is overall enhanced at higher stimulation frequencies, possibly because the inhibitory response following a stimulus is still in effect when the next stimulus is administered in a train of stimulation at 8 Hz but not as 4 Hz. Indeed, one of the explanations proposed by Wang et al (2013) is that the effect of inhibition runs longer than that of the excitation, and therefore the subsequent excitation in a train overlaps the inhibition. It was also shown that a decrease in the firing of neurons to high-frequency stimuli is a consequence of an altered balance in excitatory and inhibitory cortical activity (House et al 2011, Li et al 2009).

Our findings in mice experiments differ from Fukuda et al. (2013)'s findings in SD rat experiments. Fukuda et al. (2013) reported that under dexmedetomidine sedation (with the addition of pancuronium bromide) the evoked LFP and CBF responses to forepaw stimulation were larger at a frequency of 8–10 Hz than those elicited by 4 Hz, 6 Hz, and 12 Hz stimulation.

The difference in the stimulus frequency dependence of the LFP responses between mice and SD rats suggests that the effect of stimulus frequency on the balance between excitation and inhibition is different for these two species.

It is generally accepted that epileptic events consist of synchronous, rhythmic firing of a population of pathologically interconnected neurons capable of generating high-frequency oscillations (Bragin et al., 2002; Shariff et al., 2006). Each physiological increase in neuronal activity increases the cerebral metabolic rate of oxygen consumption, leading to an increase in CBF and CBV as the brain attempts to perfuse sufficiently the active neurons with oxygenated hemoglobin (Schwartz and Bonhoeffer, 2001; Shariff et al., 2006; Zhao et al., 2008). The signaling molecules such as adenosine and nitric oxide are released by the firing neurons, causing nearby pial arterioles to dilate (Haglund and Hochman, 2007). Consequently, seizures elicit a large focal increase in metabolism, utilization of oxygen and glucose resulting in an enormous increase in blood volume and flow to the ictal focus to provide adequate oxygenation (Engel et al., 1982; Harris et al., 2018; Patel et al., 2013). It was demonstrated that during pilocarpine-induced status epilepticus a compensation phase lasting up to 30 min is observed with an acute increase in CBF, followed by a decompensation phase with CBF decrease (Choy et al., 2010; Lothman, 1990; Reddy and Kuruba, 2013). There is a preferential distribution of blood flow to certain regions of the brain during seizures. The degree of perfusion change in the cortex is greater than in the thalamus and the hippocampus is hypo-perfused when compared to the cortex (Choy et al., 2010). In the present experiment, an increase in cerebral hemodynamics is observed during seizures simultaneously with an increase in neuronal activity. However, cerebral hemodynamics persists longer than the electrographic seizures observed in LFPs. This goes along with other findings showing that a persistent late focal hemodynamic response follows the termination of triggered ictal discharges

or spontaneous seizures (Ma et al., 2009; Zhao et al., 2007). The findings reported here are in agreement with previous studies that addressed the effects of cerebral hemodynamics during the seizures. It was reported that impaired neurovascular coupling is present in pathologic states such as epilepsy and that partial seizures have widespread effects on cortical function and cerebral perfusion (Harris et al., 2014; Zhao et al., 2007).

CONCLUSION

The findings we report, confirm that spatially extensive and high-amplitude hemodynamic responses to potent stimuli observed during brain imaging experiments that use dexmedetomidine are possibly due to the induction of epileptic activity. The choice of anesthetics and level of anesthesia are important to ensure maintaining physiological neuronal activity and hemodynamic response. It was previously shown that the hemodynamic responses of the epileptic brain follow patterns similar to those observed during normal cortical processing, except for the dip in hemoglobin oxygenation that becomes larger and more consistent during seizures (Shariff et al., 2006). Therefore, the determination of stimulation strength is critical to prevent seizures in studies of neurovascular coupling.

Moreover, the choice of the rat and mouse strains is important as they show diverse susceptibility to seizure-induction (Ferraro et al., 1995; Golden et al., 1995; McKhann et al., 2003). Our results reveal that seizures can be induced in SD and LE rats, but not in wild type, C57 mice.

Whereas, dexmedetomidine induces cerebral vasoconstriction (Jonckers et al., 2015) and decreases seizure threshold (Oishi and Suenaga, 1982), combining dexmedetomidine with isoflurane constitutes an attractive anesthesia regime for fMRI studies because both cortical and striatal functional connectivity can be reliably detected with no adverse side effects. Dexmedetomidine and isoflurane provide a synergistic effect as they exert rather opposing effects on the cerebrovascular system, isoflurane acting as vasodilator and medetomidine as vasoconstrictor (Fukuda et al., 2013; Grandjean et al., 2014).

REFERENCES

Adamczak, J.M., Farr, T.D., Seehafer, J.U., Kalthoff, D., Hoehn, M., 2010. High field BOLD response to forepaw stimulation in the mouse. Neuroimage 51, 704-712.

Airaksinen, A.M., Hekmatyar, S.K., Jerome, N., Niskanen, J.P., Huttunen, J.K., Pitkanen, A., Kauppinen, R.A., Grohn, O.H., 2012. Simultaneous BOLD fMRI and local field potential measurements during kainic acid-induced seizures. Epilepsia 53, 1245-1253.

Airaksinen, A.M., Niskanen, J.P., Chamberlain, R., Huttunen, J.K., Nissinen, J., Garwood, M., Pitkanen, A., Grohn, O., 2010. Simultaneous fMRI and local field potential measurements during epileptic seizures in medetomidine-sedated rats using raser pulse sequence. Magn Reson Med 64, 1191-1199.

Barton, M.E., Klein, B.D., Wolf, H.H., White, H.S., 2001. Pharmacological characterization of the 6 Hz psychomotor seizure model of partial epilepsy. Epilepsy Res 47, 217-227.

Boas, D.A., Dunn, A.K., 2010. Laser speckle contrast imaging in biomedical optics. J Biomed Opt 15, 011109.

Bortel, A., Yao, Z.S., Shmuel, A., 2019. A rat model of somatosensory-evoked reflex seizures induced by peripheral stimulation. Epilepsy Res 157, 106209.

Bragin, A., Mody, I., Wilson, C.L., Engel, J., Jr., 2002. Local generation of fast ripples in epileptic brain. J Neurosci 22, 2012-2021.

Bukhari, Q., Schroeter, A., Cole, D.M., Rudin, M., 2017. Resting State fMRI in Mice Reveals Anesthesia Specific Signatures of Brain Functional Networks and Their Interactions. Front Neural Circuits 11, 5.

Chaitanya, G., Arivazhagan, A., Sinha, S., Reddy, K.R., Thennarasu, K., Bharath, R.D., Rao, M.B., Chandramouli, B.A., Satishchandra, P., 2015. Dexmedetomidine anesthesia enhances spike generation during intra-operative electrocorticography: A promising adjunct for epilepsy surgery. Epilepsy Res 109, 65-71.

Choy, M., Wells, J.A., Thomas, D.L., Gadian, D.G., Scott, R.C., Lythgoe, M.F., 2010. Cerebral blood flow changes during pilocarpine-induced status epilepticus activity in the rat hippocampus. Exp Neurol 225, 196-201.

Deonna, T., 1998. Reflex seizures with somatosensory precipitation. Clinical and electroencephalographic patterns and differential diagnosis, with emphasis on reflex myoclonic epilepsy of infancy. Adv Neurol 75, 193-206.

Dunn, A.K., Bolay, H., Moskowitz, M.A., Boas, D.A., 2001. Dynamic imaging of cerebral blood flow using laser speckle. J Cereb Blood Flow Metab 21, 195-201.

Engel, J., Jr., Kuhl, D.E., Phelps, M.E., 1982. Patterns of human local cerebral glucose metabolism during epileptic seizures. Science 218, 64-66.

Esneault, E., Peyon, G., Castagne, V., 2017. Efficacy of anticonvulsant substances in the 6Hz seizure test: Comparison of two rodent species. Epilepsy Res 134, 9-15.

Ferraro, T.N., Golden, G.T., Smith, G.G., Berrettini, W.H., 1995. Differential susceptibility to seizures induced by systemic kainic acid treatment in mature DBA/2J and C57BL/6J mice. Epilepsia 36, 301-307.

Ferraro, T.N., Golden, G.T., Smith, G.G., DeMuth, D., Buono, R.J., Berrettini, W.H., 2002. Mouse strain variation in maximal electroshock seizure threshold. Brain Res 936, 82-86.

Fox, M.D., Greicius, M., 2010. Clinical applications of resting state functional connectivity. Front Syst Neurosci 4, 19.

Frankel, W.N., Taylor, L., Beyer, B., Tempel, B.L., White, H.S., 2001. Electroconvulsive thresholds of inbred mouse strains. Genomics 74, 306-312.

Franklin, K., Paxinos, G., 2007. The Mouse Brain in Stereotaxic Coordinates, 3rd ed. Elsevier Academic Press, New York.

Friston, K.J., Frith, C.D., Liddle, P.F., Frackowiak, R.S., 1993. Functional connectivity: the principal-component analysis of large (PET) data sets. J Cereb Blood Flow Metab 13, 5-14.

Fukuda, M., Vazquez, A.L., Zong, X., Kim, S.G., 2013. Effects of the alpha(2)-adrenergic receptor agonist dexmedetomidine on neural, vascular and BOLD fMRI responses in the somatosensory cortex. Eur J Neurosci 37, 80-95.

Gertler, R., Brown, H.C., Mitchell, D.H., Silvius, E.N., 2001. Dexmedetomidine: a novel sedative-analgesic agent. Proc (Bayl Univ Med Cent) 14, 13-21.

Golden, G.T., Smith, G.G., Ferraro, T.N., Reyes, P.F., 1995. Rat strain and age differences in kainic acid induced seizures. Epilepsy Res 20, 151-159.

Grandjean, J., Schroeter, A., Batata, I., Rudin, M., 2014. Optimization of anesthesia protocol for resting-state fMRI in mice based on differential effects of anesthetics on functional connectivity patterns. Neuroimage 102 Pt 2, 838-847.

Grinvald, A., Shoham, D., Shmuel, A., Glaser, D., Vanzetta, I., Shtoyerman, E., Slovin, H., Sterkin, A., Wijnbergen, C., Hildesheim, R., 1999. Modern techniques in neuroscience research. In-vivo Optical Imaging of cortical Architecture and Dynamics. Springer, 893.

Haglund, M.M., Hochman, D.W., 2007. Imaging of intrinsic optical signals in primate cortex during epileptiform activity. Epilepsia 48 Suppl 4, 65-74.

Halonen, T., Kotti, T., Tuunanen, J., Toppinen, A., Miettinen, R., Riekkinen, P.J., 1995. Alpha 2-adrenoceptor agonist, dexmedetomidine, protects against kainic acid-induced convulsions and neuronal damage. Brain Res 693, 217-224.

Harris, S., Boorman, L., Bruyns-Haylett, M., Kennerley, A., Ma, H., Zhao, M., Overton, P.G., Schwartz, T.H., Berwick, J., 2014. Contralateral dissociation between neural activity and cerebral blood volume during recurrent acute focal neocortical seizures. Epilepsia 55, 1423-1430.

Harris, S.S., Boorman, L.W., Kennerley, A.J., Sharp, P.S., Martin, C., Redgrave, P., Schwartz, T.H., Berwick, J., 2018. Seizure epicenter depth and translaminar field potential synchrony underlie complex variations in tissue oxygenation during ictal initiation. Neuroimage 171, 165-175.

House, D.R., Elstrott, J., Koh, E., Chung, J., Feldman, D.E., 2011. Parallel regulation of feedforward inhibition and excitation during whisker map plasticity. Neuron 72, 819-831.

Hsieh, C.Y., Chiou, N.J., Wu, Y.J., Tsai, J.J., Huang, C.W., 2011. Somatosensory rub evoked reflex epilepsy of a temporal lobe origin. Neurol Sci 32, 297-299.

Huttunen, J.K., Grohn, O., Penttonen, M., 2008. Coupling between simultaneously recorded BOLD response and neuronal activity in the rat somatosensory cortex. Neuroimage 39, 775-785.

Jonckers, E., Shah, D., Hamaide, J., Verhoye, M., Van der Linden, A., 2015. The power of using functional fMRI on small rodents to study brain pharmacology and disease. Front Pharmacol 6, 231.

Kan, M.C., Wang, W.P., Yao, G.D., Li, J.T., Xie, T., Wang, W., Ma, W.Q., 2013. Anticonvulsant effect of dexmedetomidine in a rat model of self-sustaining status epilepticus with prolonged amygdala stimulation. Neurosci Lett 543, 17-21.

Kanemoto, K., Watanabe, Y., Tsuji, T., Fukami, M., Kawasaki, J., 2001. Rub epilepsy: a somatosensory evoked reflex epilepsy induced by prolonged cutaneous stimulation. J Neurol Neurosurg Psychiatry 70, 541-543.

Kim, T., Masamoto, K., Fukuda, M., Vazquez, A., Kim, S.G., 2010. Frequency-dependent neural activity, CBF, and BOLD fMRI to somatosensory stimuli in isoflurane-anesthetized rats. Neuroimage 52, 224-233.

Krautwald, K., Angenstein, F., 2012. Low frequency stimulation of the perforant pathway generates anesthesia-specific variations in neural activity and BOLD responses in the rat dentate gyrus. J Cereb Blood Flow Metab 32, 291-305.

Li, P., Rudolph, U., Huntsman, M.M., 2009. Long-term sensory deprivation selectively rearranges functional inhibitory circuits in mouse barrel cortex. Proc Natl Acad Sci U S A 106, 12156-12161.

Lothman, E., 1990. The biochemical basis and pathophysiology of status epilepticus. Neurology 40, 13-23.

Ma, H., Zhao, M., Suh, M., Schwartz, T.H., 2009. Hemodynamic surrogates for excitatory membrane potential change during interictal epileptiform events in rat neocortex. J Neurophysiol 101, 2550-2562.

Magnuson, M.E., Thompson, G.J., Pan, W.J., Keilholz, S.D., 2014. Time-dependent effects of isoflurane and dexmedetomidine on functional connectivity, spectral characteristics, and spatial distribution of spontaneous BOLD fluctuations. NMR Biomed 27, 291-303.

Masamoto, K., Kim, T., Fukuda, M., Wang, P., Kim, S.G., 2007. Relationship between neural, vascular, and BOLD signals in isoflurane-anesthetized rat somatosensory cortex. Cereb Cortex 17, 942-950.

McKhann, G.M., 2nd, Wenzel, H.J., Robbins, C.A., Sosunov, A.A., Schwartzkroin, P.A., 2003. Mouse strain differences in kainic acid sensitivity, seizure behavior, mortality, and hippocampal pathology. Neuroscience 122, 551-561.

Mirski, M.A., Rossell, L.A., McPherson, R.W., Traystman, R.J., 1994. Dexmedetomidine decreases seizure threshold in a rat model of experimental generalized epilepsy. Anesthesiology 81, 1422-1428.

Nasrallah, F.A., Tan, J., Chuang, K.H., 2012. Pharmacological modulation of functional connectivity: alpha2-adrenergic receptor agonist alters synchrony but not neural activation. Neuroimage 60, 436-446.

Oishi, R., Suenaga, N., 1982. The role of the locus coeruleus in regulation of seizure susceptibility in rats. Jpn J Pharmacol 32, 1075-1081.

Paasonen, J., Stenroos, P., Salo, R.A., Kiviniemi, V., Grohn, O., 2018. Functional connectivity under six anesthesia protocols and the awake condition in rat brain. Neuroimage 172, 9-20.

Panayiotopoulos, C.P., 2005. Reflex Seizures and Reflex Epilepsies. In: Panayiotopoulos, C.P. (Ed.), The Epilepsies: Seizures, Syndromes and Management. Bladon Medical Publishing, Oxfordshire (UK).

Patel, K.S., Zhao, M., Ma, H., Schwartz, T.H., 2013. Imaging preictal hemodynamic changes in neocortical epilepsy. Neurosurg Focus 34, E10.

Pawela, C.P., Biswal, B.B., Cho, Y.R., Kao, D.S., Li, R., Jones, S.R., Schulte, M.L., Matloub, H.S., Hudetz, A.G., Hyde, J.S., 2008. Resting-state functional connectivity of the rat brain. Magn Reson Med 59, 1021-1029.

Pawela, C.P., Biswal, B.B., Hudetz, A.G., Schulte, M.L., Li, R., Jones, S.R., Cho, Y.R., Matloub, H.S., Hyde, J.S., 2009. A protocol for use of medetomidine anesthesia in rats for extended studies using task-induced BOLD contrast and resting-state functional connectivity. Neuroimage 46, 1137-1147.

Paxinos, G., Watson, C., 2005. The rat brain in stereotaxic coordinates., 5th ed. Elsevier Academic Press, Boston.

Reddy, D.S., Kuruba, R., 2013. Experimental models of status epilepticus and neuronal injury for evaluation of therapeutic interventions. Int J Mol Sci 14, 18284-18318.

Sala-Padro, J., Toledo, M., Sarria, S., Santamarina, E., Gonzalez-Cuevas, M., Sueiras-Gil, M., Salas-Puig, J., 2015. Reflex seizures triggered by cutaneous stimuli. Seizure 33, 72-75.

Schauwecker, P.E., 2002. Complications associated with genetic background effects in models of experimental epilepsy. Prog Brain Res 135, 139-148.

Schwartz, T.H., Bonhoeffer, T., 2001. In vivo optical mapping of epileptic foci and surround inhibition in ferret cerebral cortex. Nat Med 7, 1063-1067.

Shariff, S., Suh, M., Zhao, M., Ma, H., Schwartz, T.H., 2006. Recent developments in oximetry and perfusion-based mapping techniques and their role in the surgical treatment of neocortical epilepsy. Epilepsy Behav 8, 363-375.

Shmuel, A., Leopold, D.A., 2008. Neuronal correlates of spontaneous fluctuations in fMRI signals in monkey visual cortex: Implications for functional connectivity at rest. Hum Brain Mapp 29, 751-761.

Sotero, R.C., Bortel, A., Martínez-Cancino, R., Neupane, S., O'Connor, P., Carbonell, F., Shmuel, A. (2010) Anatomically-constrained effective connectivity among layers in a cortical column modeled and estimated from local field potentials. Journal of Integrative Neuroscience 9, 355–379.

Sotero, R.C., Bortel, A., Naaman, S., Mocanu, V.M., Kropf, P., Villeneuve, M.Y., Shmuel, A., 2015. Laminar Distribution of Phase-Amplitude Coupling of Spontaneous Current Sources and Sinks. Front Neurosci 9, 454.

Striano, S., Coppola, A., del Gaudio, L., Striano, P., 2012. Reflex seizures and reflex epilepsies: old models for understanding mechanisms of epileptogenesis. Epilepsy Res 100, 1-11.

Turrigiano, G., 2011. Too many cooks? Intrinsic and synaptic homeostatic mechanisms in cortical circuit refinement. Annu Rev Neurosci 34, 89-103.

Wang, Z., Qi, H.X., Kaas, J.H., Roe, A.W., Chen, L.M., 2013. Functional signature of recovering cortex: dissociation of local field potentials and spiking activity in somatosensory cortices of spinal cord injured monkeys. Exp Neurol 249, 132-143.

Weber, R., Ramos-Cabrer, P., Wiedermann, D., van Camp, N., Hoehn, M., 2006. A fully noninvasive and robust experimental protocol for longitudinal fMRI studies in the rat. Neuroimage 29, 1303-1310.

Whittington, R.A., Virag, L., Vulliemoz, Y., Cooper, T.B., Morishima, H.O., 2002. Dexmedetomidine increases the cocaine seizure threshold in rats. Anesthesiology 97, 693-700.

Wolf, P., 2015. Reflex epileptic mechanisms in humans: Lessons about natural ictogenesis. Epilepsy Behav.

Zhao, F., Zhao, T., Zhou, L., Wu, Q., Hu, X., 2008. BOLD study of stimulation-induced neural activity and resting-state connectivity in medetomidine-sedated rat. Neuroimage 39, 248-260.

Zhao, M., Suh, M., Ma, H., Perry, C., Geneslaw, A., Schwartz, T.H., 2007. Focal increases in perfusion and decreases in hemoglobin oxygenation precede seizure onset in spontaneous human epilepsy. Epilepsia 48, 2059-2067.

FIGURE LEGENDS

Figure 1. Forepaw stimulation induces epileptic activity in rat area S1FL. A. LFP recordings of ten trials, each with 10s-long stimulation. The stimulation periods are marked by black rectangles. Each 10s stimulus consisted of a train of electrical pulses delivered at 8 Hz to the forepaw. Note that during the first, fourth, and seventh trials, the stimulation evoked a seizure. **B.** Top: The LFP (mean averaged over electrode contacts spanning the cortical depth) demonstrates a normal-evoked response in trial #3. Bottom: The corresponding spectrogram (power as a function of frequency and time) computed for the same trial. **C.** Top: LFP (mean averaged over

electrode contacts spanning the cortical depth) showing a seizure pattern in trial #4. The red and green arrows indicate the onset and termination, respectively, of a seizure induced by forepaw stimulation. Bottom: The corresponding spectrogram, computed for the same seizure. D. The number of evoked seizures per rat as a function of time shows that seizures were induced already during the first or the second run, only one hour after initiating the dexmedetomidine sedation.

Figure 2. Cerebral blood oxygenation responses evoked by forepaw stimulation. A. Cerebral blood oxygenation response evoked by stimulation of the contralateral forepaw. To the left, the spatial responses before (the 1s before stimulus onset), during (9-10s following stimulus onset), and after (9-10s following the cessation of the stimulus) the 10s-long forepaw stimulation period. The reference for obtaining these responses was imaged between 3 and 1 seconds before stimulus onset. Note that positive response indicated in indexed yellow and red colors represent an increase in blood oxygenation. To the right are two time-courses presenting the corresponding temporal response from two regions (blue and red ROIs in panel C) within the activated area. The stimulation period between 0 and 10 seconds is marked by a dark bar. **B.** Maps of the blood oxygenation changes during a response that evoked a seizure, from before, during, and after the 10s-long forepaw stimulation period (exact time periods are as in A). To the right are two time-courses presenting the corresponding temporal response from two regions (blue and red ROIs in panel C) within the activated area. **C.** The imaged cortical surface with the two ROIs used for sampling the time-courses presented in A and B.

Figure 3. Cerebral blood flow responses evoked by forepaw stimulation. A. Cerebral blood flow response evoked by stimulation of the contralateral forepaw. To the left, the spatial responses before (the 1s before stimulus onset), during (9-10s following stimulus onset), and after (9-10s following the cessation of the stimulus) the 10s-long forepaw stimulation period. The reference for obtaining these responses was imaged between 3 and 1 seconds before stimulus onset. Note that positive responses indicated in indexed yellow and red colors represent an increase in blood flow. To the right are two time-courses presenting the corresponding temporal response from two regions (blue and red ROIs in Figure 2C) within the activated area. The stimulation period between 0 and 10 seconds is marked by a dark bar. **B.** Maps of the blood flow changes during a response that evoked a seizure, from before, during, and after the 10s-long forepaw stimulation period (exact time periods are as in A). To the right are two time-courses presenting the corresponding temporal response from the same ROIs as described in A. **C.** A bar graph showing the spatial extent of the CBF response calculated for the epochs of 5-10s, 10-15s, and 15-20s relative to the onset of the stimulus during normal evoked responses (n=21), seizure responses (n=20) and refractory periods (n=14; * $p<0.05$, ** $p<0.001$; Tamhane's test).

Figure 4. Forepaw stimulation induces epileptic activity in LE rat. A. LFP recordings of ten trials, each with 10s-long stimulation. The stimulation periods are marked by black rectangles. Note that during the first, third, fifth, sixth, eight and ninth trials, the stimulation induced a seizure. **B.** Top: The LFP (mean averaged over electrode contacts spanning the cortical depth) demonstrates a normal-evoked response in trial #7. Bottom: The corresponding spectrogram

(power as a function of frequency and time) computed for the same trial. **C.** Top: LFP (mean averaged over electrode contacts spanning the cortical depth) showing a seizure pattern in trial #9. The red and green arrows indicate the onset and termination, respectively, of a seizure induced by forepaw stimulation. Bottom: The corresponding spectrogram, computed for the same seizure. D. The number of evoked seizures per rat as a function of time shows that seizures are induced already during the first or the third run, only one hour after initiating dexmedetomidine sedation.

Figure 5. Absence of seizures in the C57BL6 mouse strain. **A.** Top: Normal LFP responses obtained from area S1FL, in response 4Hz forepaw stimulation. The panel shows ten trials, each with 10s-long stimulation. The stimulation blocks are marked by black rectangles. Bottom: A magnification of the normal evoked response from the first trial. **B.** Top: Normal LFP responses to 6Hz forepaw stimulation. Bottom: A magnification of the normal evoked response from the first trial. **C.** Top: A typical activity pattern of evoked responses to 8Hz forepaw stimulation. Bottom: A magnification of the normal evoked response from the third trial.

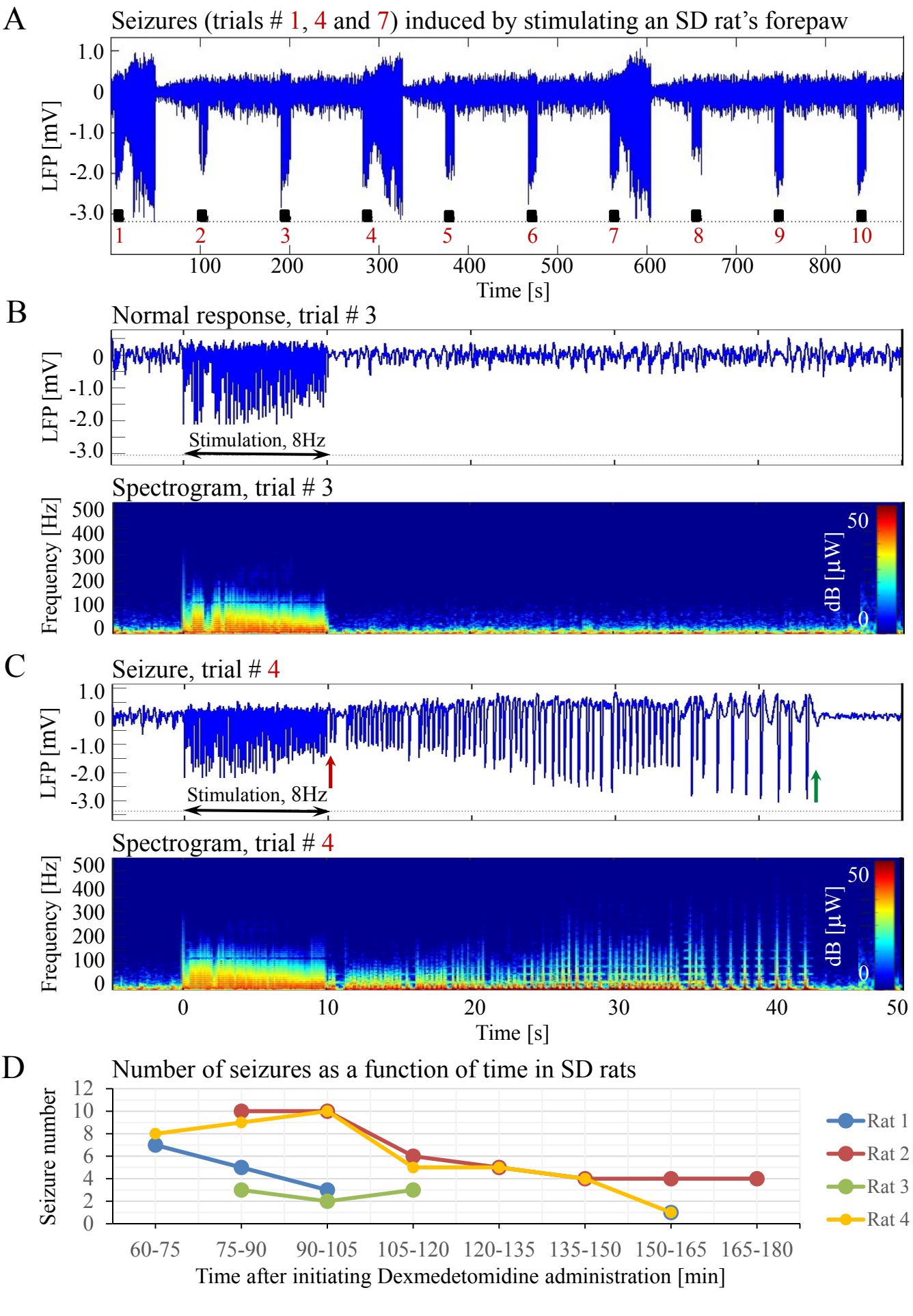

Blood oxygenation responses to forepaw stimulation

A Oxy-hemoglobin response associated with a normal evoked response

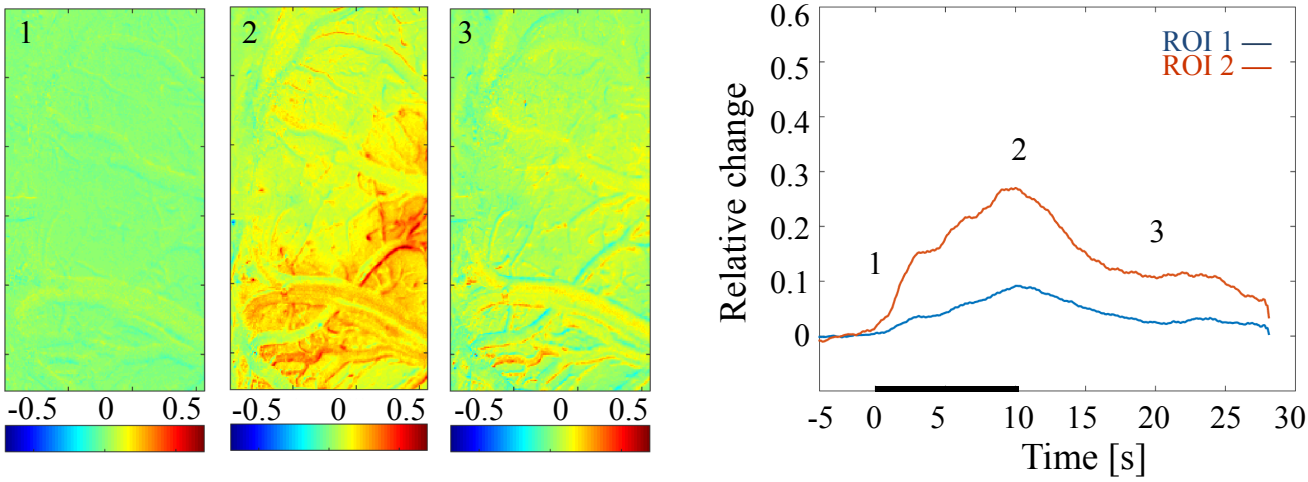

B Oxy-hemoglobin response associated with a seizure

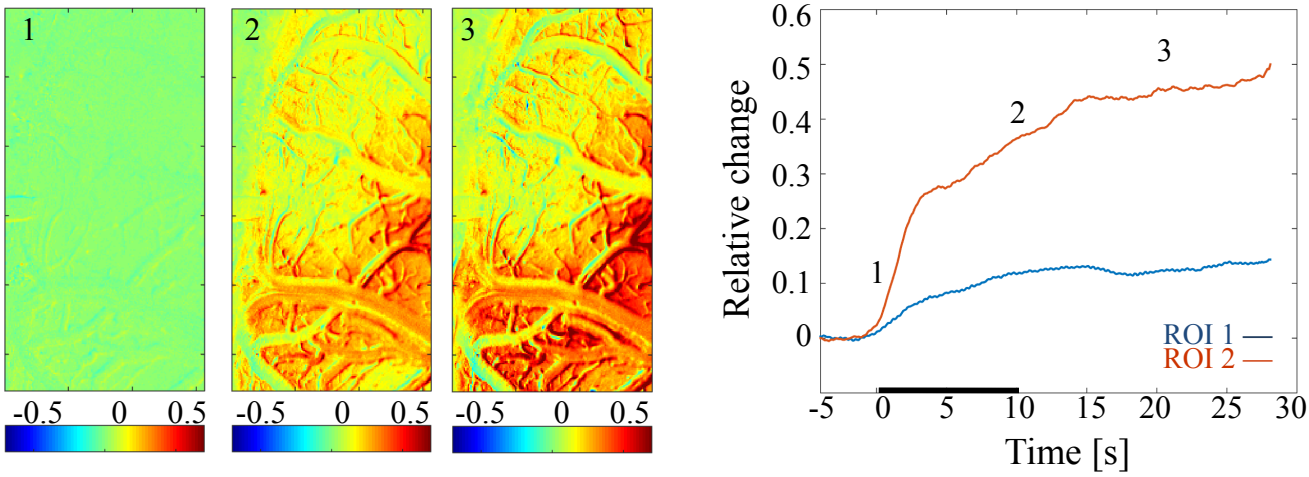

C Surface of the brain

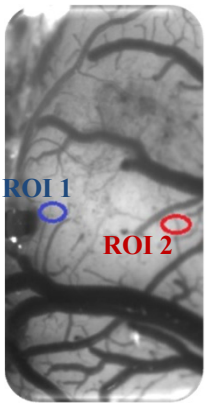

Figure 2

Cerebral blood flow responses to forepaw stimulation

A Cerebral blood flow response associated with a normal evoked response

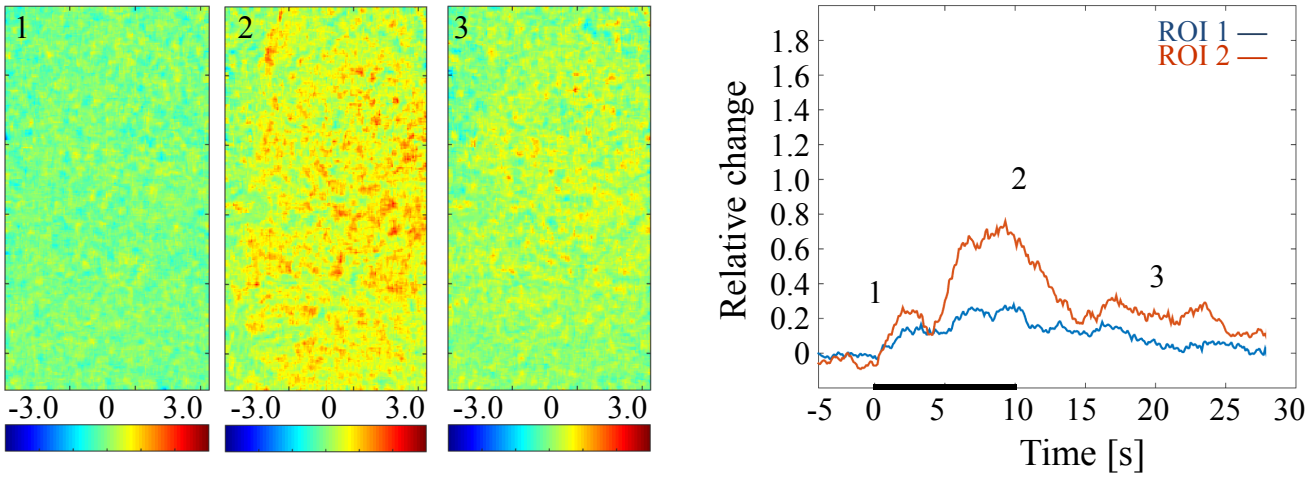

B Cerebral blood flow response associated with a seizure

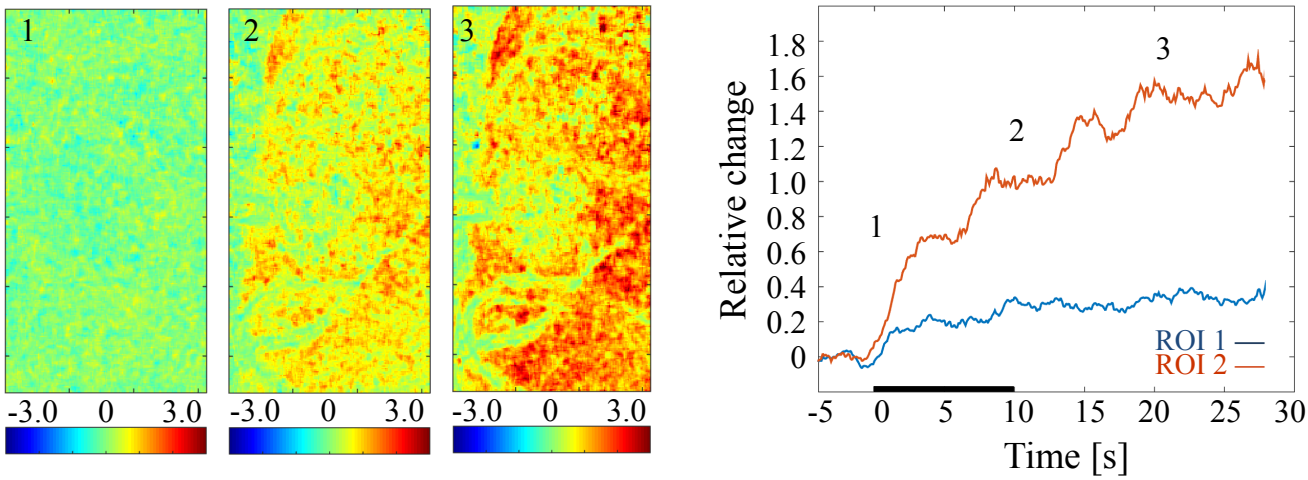

C Spatial extent of active area - CBF

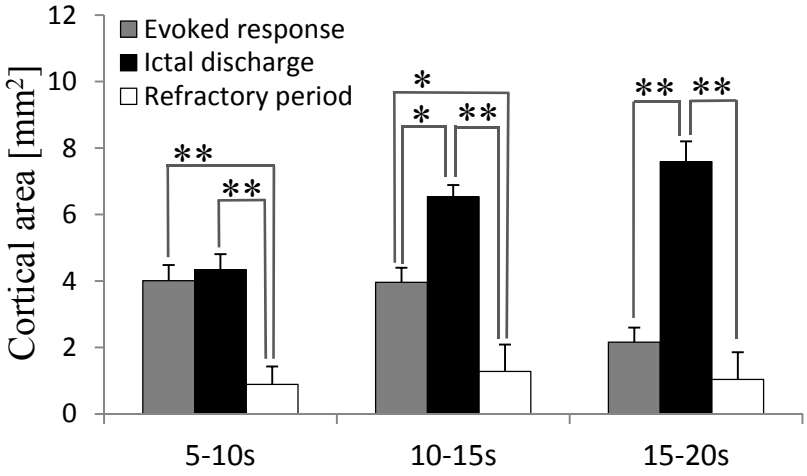

Figure 3

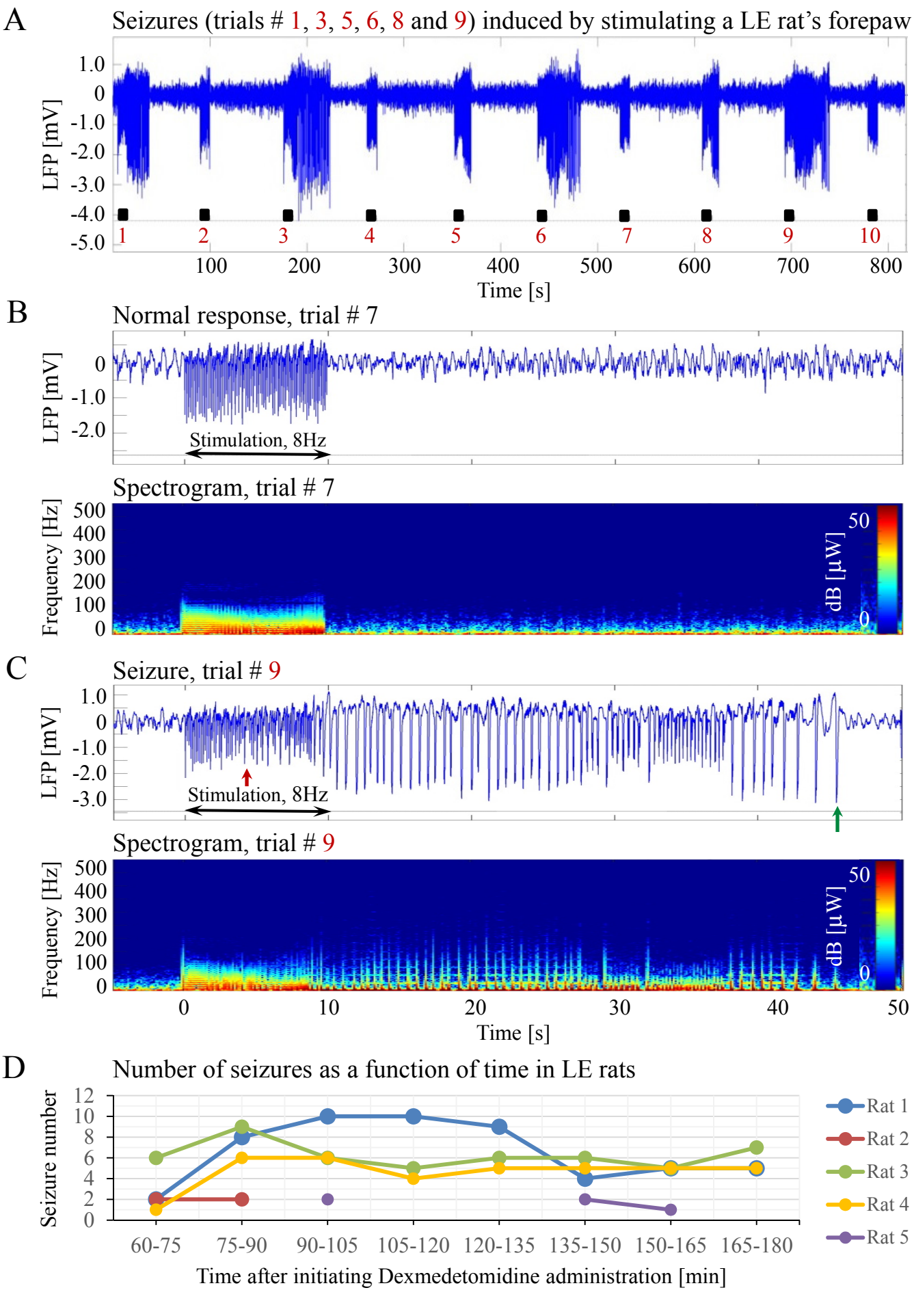

A

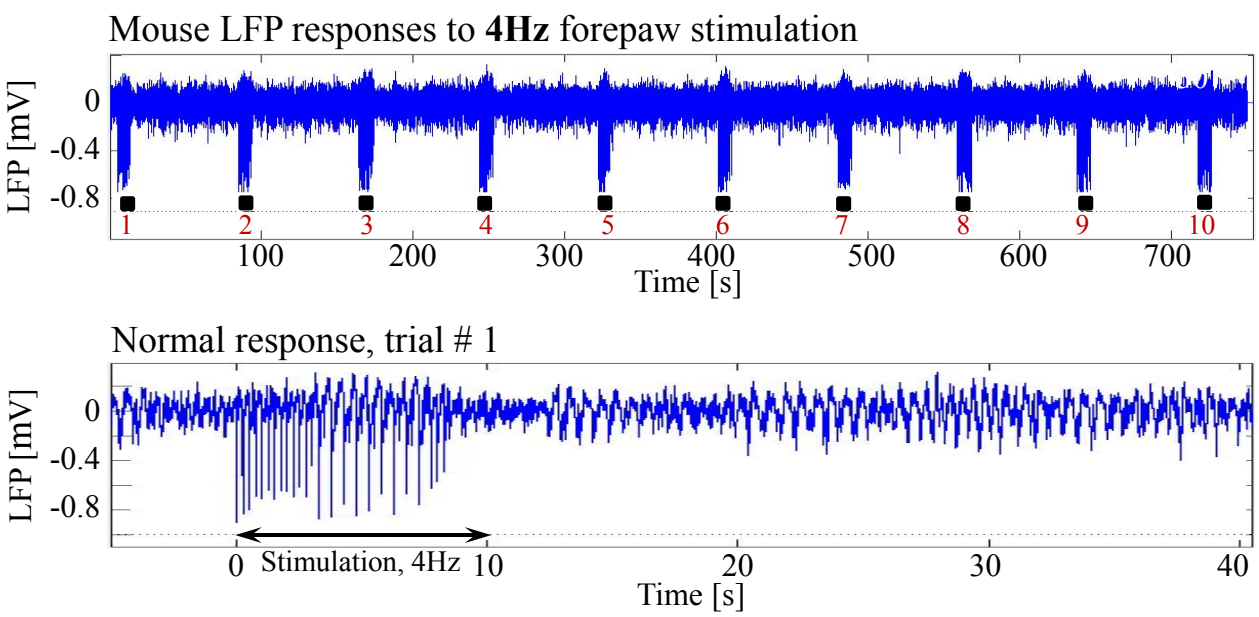

B

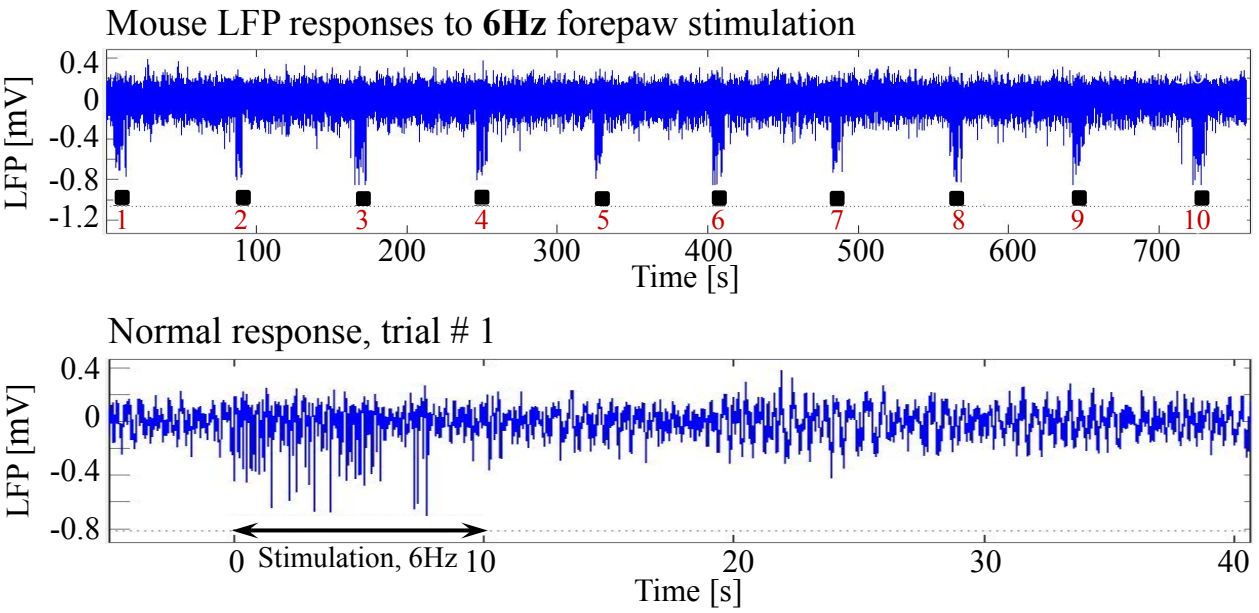

C